Analytic Study of Rotating Black-Hole Quasinormal Modes

Uri Keshet
Institute for Advanced Study, Einstein Drive, Princeton, NJ 08540, USA *

Shahar Hod
The Ruppin Academic Center, Emeq Hefer 40250, Israel
and The Hadassah Institute, Jerusalem 91010, Israel
(Dated: February 1, 2008)

A Bohr-Sommerfeld equation is derived for the highly-damped quasinormal mode frequencies $\omega(n \gg 1)$ of rotating black holes. It may be written as $2\int_C (p_r + ip_0)\, dr = (n+1/2)h$, where p_r is the canonical momentum conjugate to the radial coordinate r along a null geodesic of energy $\hbar\omega$ and angular momentum $\hbar m$, $p_0 = O(\omega^0)$, and the contour C connects two complex turning points of p_r. The solutions are $\omega(n) = -m\widehat{\omega} - i(\widehat{\phi} + n\widehat{\delta})$, where $\{\widehat{\omega}, \widehat{\delta}\} > 0$ are functions of the black-hole parameters alone. Some physical implications are discussed.

PACS numbers: 04.70.Bw, 03.65.Pm, 04.30.-w, 04.70.Dy

Quantizing black holes may become an important step towards quantum gravity, analogous to the role played by atomic models in the development of quantum mechanics. Thus, the "no-hair" conjecture [1] suggests that in a quantum theory of gravity, a black hole may be described by few quantum numbers related to its mass M, electric charge Q, and angular momentum J. The existence of classically reversible changes in the state of a nonextremal black hole [2] suggests that its area A is an adiabatic invariant, possibly corresponding to a quantum entity with a discrete spectrum [3].

Classical black holes, like most systems with radiative boundary conditions, are characterized by a discrete set of complex ringing frequencies $\omega(n) = \omega_R + i\omega_I$ known as quasinormal modes (QNMs) [4]. In the spirit of Bohr's correspondence principle, the classical QNM spectrum of a black-hole should be reproduced as resonances in a quantum theory of gravity. QNM spectroscopy may thus provide valuable clues towards such a theory. In particular, the asymptotically damped frequency $\widetilde{\omega}_R \equiv \omega_R(n \to \infty)$, which for a spherically-symmetric black hole depends only on the black hole parameters [e.g. 5], may have a simple counterpart in quantum gravity [6]. Indeed, for a Schwarzschild black hole $\widetilde{\omega}_R = (8\pi M)^{-1}\ln 3$, such that the change in black hole entropy associated with $\Delta M = \hbar\widetilde{\omega}_R$, $\Delta S = \Delta(4\pi M^2/\hbar) = \ln 3$, admits a (triply-) degenerate quantum-state interpretation [6, 7]. We use geometrized units where $G = c = k_B = 1$.

Although $\widetilde{\omega}$ was analytically derived for spherically symmetric black holes [5, 7], little is known about the generic and more complicated case of rotating black holes. Contradicting results for $\widetilde{\omega}$ have appeared in the literature, although numerical convergence has recently been reported [8]. An analytical solution is essential in order to test and physically interpret these results.

We analytically derive $\widetilde{\omega}$ for rotating black holes in a method similar to the spherical black-hole analysis of [5], by analytically continuing the relevant solution of Teukolsky's radial equation [9] to the complex plane, and matching the monodromy of the wave-function along two different contours. Our analytical results confirm and generalize the numerical results of [8], as well as admit a physical interpretation. In this Rapid Communication we outline the derivation and present the main results, deferring a more elaborate description of the analysis to a future, detailed paper.

Teukolsky's equation.— Linear, massless field perturbations of a neutral, rotating black hole are described by Teukolsky's equation. For a scalar field, this equation can be generalized to accommodate electrically charged black holes [10]; in what follows, $Q \neq 0$ is understood to apply only to such fields. The wave-function is separated into two ordinary differential equations using $\psi(x) = e^{i(m\phi - \omega t)} S_{lm}(\cos\theta) R_{lm}(r)$, where $x = (t, r, \theta, \phi)$ are Boyer-Lindquist coordinates. This yields radial and angular equations coupled by a separation constant A_{lm}, where $A_{lm}(\omega_I \to -\infty) = iA_1 a\omega + (A_0 + m^2) + O(|\omega|^{-1})$, with $A_1 \in \mathbb{R}$ [8, 11]. The radial equation then becomes

$$\left[\frac{\partial^2}{\partial r^2} + \frac{q_0(r)\omega^2 + q_1(r)\omega + q_2(r)}{\Delta^2}\right] \widetilde{R}_{lm} = 0 \ , \qquad (1)$$

where $\widetilde{R}_{lm} \equiv \Delta^{(s+1)/2} R_{lm}$, $\Delta \equiv r^2 - 2Mr + a^2 + Q^2$, $a \equiv J/M$, and we have defined

$$q_0 \equiv (r^2 + a^2)^2 - a^2\Delta \ , \qquad (2)$$

$$\begin{aligned} q_1 \ \equiv\ & -2am(2Mr - Q^2) - iaA_1\Delta \\ & +2is[r(\Delta + Q^2) - M(r^2 - a^2)] \ , \end{aligned} \qquad (3)$$

and

$$\begin{aligned} q_2 \ \equiv\ & -m^2(\Delta - a^2) - \Delta(s + A_0) + M^2 - a^2 - Q^2 \\ & -s(M - r)[2iam + s(M - r)] \ . \end{aligned} \qquad (4)$$

---

*Friends of the Institute for Advanced Study member; Electronic address: keshet@sns.ias.edu

The spin-weight parameter s specifies the equation to gravitational ($s = -2$), electromagnetic ($s = -1$), scalar ($s = 0$), or two-component neutrino ($s = -1/2$) fields. For physical boundary conditions of purely outgoing waves at both spatial infinity and the event horizon (i.e. crossing the horizon into the black hole), Eq. (1) admits solutions only for a discrete set of QNM frequencies $\omega(n)$, where $\omega_I < 0$ (time decay) diverges as $n \to \infty$.

Analysis.— By defining $z \equiv \int^r V(r')dr'$, with $V \equiv \Delta^{-1}(q_0 + \omega^{-1} q_1)^{1/2}$, Eq. (1) becomes

$$\left(-\frac{\partial^2}{\partial z^2} + V_1 - \omega^2\right)\widehat{R} = 0 \;, \qquad (5)$$

where $\widehat{R} = V^{1/2}\widetilde{R}$ and $V_1 = V''/(2V^3) - 3(V')^2/(4V^4) - q_2/(V\Delta)^2$. A nonconventional tortoise coordinate z was defined such that the effective potential $V_1 = O(|\omega|^0)$. The boundary condition at the horizon becomes $\widehat{R}(r \to r_+) \sim \exp(-i\omega z) \propto (r - r_+)^{-i\omega\sigma_+}$, where

$$\omega\sigma_+ = \omega \operatorname*{Res}_{r \to r_+}(V) = \beta(\omega - m\Omega) - \frac{is}{2} + O(|\omega|^{-1}) \;. \qquad (6)$$

Here, $\Omega \equiv a/(r_+^2 + a^2)$ is the angular velocity of the event horizon, $\beta \equiv \hbar/(4\pi T) = (r_+^2 + a^2)/(r_+ - r_-)$, T is the Bekenstein-Hawking temperature, $r_\pm = M \pm (M^2 - a^2 - Q^2)^{1/2}$ are the outer and inner horizon radii, and the tilde in $\widetilde{\omega}$ is omitted unless necessary (henceforth). $\widehat{R}(r \simeq r_+)$ is multivalued, such that a clockwise rotation around r_+ multiplies $\widehat{R}$ by a factor $\Phi_1 = \exp(-2\pi\omega\sigma_+)$.

Let r_1 and $r_2 = r_1^*$ be the two complex conjugate roots of $q_0(r)$ lying in the fourth and in the first quadrants, respectively. Denote t_1 and t_2 as the turning points of V [defined by $V(r = t_i) = 0$] which lie near (a factor $\sim |\omega|^{-1}$ away from) r_1 and r_2, respectively (see Figure 1). The monodromy Φ_2 of $\widehat{R}$ along a clockwise contour C, which passes through t_1 and t_2 and encloses r_+, is used to determine ω by demanding $\Phi_1 = \Phi_2$, as in [5]. A reader uninterested in details of the derivation may skip directly to the result, Eq. (8).

Near the turning points, $(z - z_i) \propto (r - t_i)^{3/2}$, where $z_i \equiv z(t_i)$. Therefore three anti-Stokes lines, defined by $\Re(i\omega z) = 0$, emanate from t_i. Two anti-Stokes lines connect t_1 to t_2; one (denoted l_2) crosses the real axis between r_- and r_+, while the other crosses it at $r > r_+$. The third anti-Stokes line (l_1) emanating from t_1 extends to P_1, where $|P_1| \to \infty$ and $\arg(P_1) = -\pi/2$. A similar line (l_3) runs from t_2 to P_2, with $|P_2| \to \infty$ and $\arg(P_2) = +\pi/2$. A Stokes line, defined by $\Im(i\omega z) = 0$, emanates between every two anti-Stokes lines of t_i. Let C be the closed, clockwise contour running from P_1 to P_2 along the anti-Stokes lines l_1, l_2 and l_3, and closing back on P_1 through the large semicircle l_∞, where $|r| \to \infty$ and $-\pi/2 < \arg(r) < \pi/2$. The turning points t_1 and t_2 are excluded from C by partially rotating around them counterclockwise. Figure 1 illustrates these features in the r-plane.

Along anti-Stokes lines, the WKB approximation $\widehat{R}(z, z_0) \;\simeq\; c_+ \exp[+i\omega(z - z_0)] + c_- \exp[-i\omega(z - z_0)]$

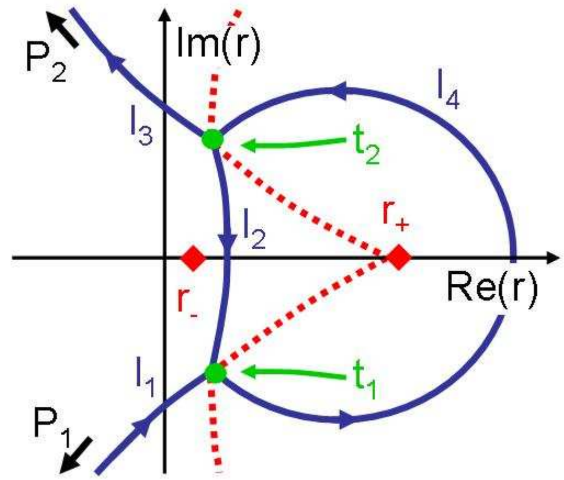

FIG. 1: Illustration of anti-Stokes (solid) and Stokes (dashed) lines emanating from the turning points t_1 and t_2 (disks) in the complex r-plane, for $a = 0.3$, $Q = 0$ in the highly damped limit. The inner and outer horizon radii (diamonds) and components of the contour C are also shown. Arrows along anti-Stokes lines denote the direction of increasing $\Im z$.

holds. Off the lines, this may also be written as $c_d f_d + c_s f_s$, where f_d is exponentially large (dominant) and f_s is exponentially small (subdominant). For $\omega_R < 0$, the boundary condition at spatial infinity can be analytically continued to P_1 [5] such that $\widehat{R}(P_1) \sim \exp(+i\omega z)$, i.e. $\{c_+, c_-; z_0\} = \{1, 0; z_1\}$ up to a multiplicative factor. This remains invariant along l_1 till the vicinity of t_1, so we denote $\widehat{R}(l_1) = \{1, 0; z_1\}$. When an anti-Stokes line is crossed, the dominant and subdominant parts exchange roles. When a Stokes line is crossed while circling a regular turning point, $c_d f_d + c_s f_s$ becomes $c_d f_d + (c_s \pm i c_d) f_d$, where the positive (negative) sign corresponds to a counterclockwise (clockwise) rotation. This so-called Stokes phenomenon [12] implies that after rotating around t_1 from l_1 to l_2, thus crossing two Stokes lines and the anti-Stokes line between them, $\widehat{R}(l_2) = \{0, i; z_1\} = \{0, i\exp(-i\omega\delta); z_2\}$, where

$$\delta \equiv z_2 - z_1 = \int_{l_2} V\, dr \;. \qquad (7)$$

Similarly, after rotating from l_2 to l_3, $\widehat{R}(l_3) = \{-\exp(-2i\omega\delta), 0; z_1\}$. Finally, along l_∞ the coefficient of the dominant part of the solution c_+ remains invariant till P_1. In addition to the above changes in c_+, it accumulates a phase $e^{+2\pi\omega\sigma_+}$ due to the (only) singularity at r_+ enclosed by C. Thus, the total phase accumulated by $\widehat{R}$ along C is $\Phi_2 = -\exp(-2i\omega\delta + 2\pi\omega\sigma_+)$. For $\omega_R > 0$, the boundary condition at spatial infinity is continued to P_2 and the two contours are chosen counterclockwise, such that the resulting equation $\Phi_1 = \Phi_2$ is unchanged.

The constraint $\Phi_1 = \Phi_2$ finally yields the highly-

damped QNM equation [16]

$$e^{-2\pi\omega\sigma_+} = -e^{-2i\omega\delta+2\pi\omega\sigma_+} \; . \tag{8}$$

Explicitly, to order $O(|\omega|^{-1})$ this may be written as

$$4\pi\beta\,(\omega - m\Omega) - 2\pi i s = 2i\omega \int_{C_{t,i}} V\, dr - \pi i(2n+1) \; , \tag{9}$$

or in a more compact form as

$$2\omega \int_{C_{t,o}} V\, dr = 2\pi \left(n + \frac{1}{2} \right) \; , \tag{10}$$

where $n \in \mathbb{Z}$. Here, $C_{t,i}$ ($C_{t,o}$) is a complex-plane contour running from t_1 to t_2, crossing the real axis in (out) of the event horizon, at some point $r_- < r < r_+$ ($r > r_+$).

Before solving for $\widetilde{\omega}$, note that in the highly-damped limit the real and the imaginary contributions to the integrals of Eqs. (7)-(10) are easily separated. For example, the real part of Eq. (9) may be written in the form [17]

$$4\pi\beta(\omega_R - m\Omega) = \Re\left(2i \int_{C_{t,i}} \omega V_R\, dr \right) \; , \tag{11}$$

where the complex potential V_R is given by

$$(\omega V_R)^2 = \frac{q_0\omega^2 - 2am(2Mr - Q^2)\omega - m^2(\Delta - a^2)}{\Delta^2} \; . \tag{12}$$

The last term ($\propto \omega^0$, taken from q_2) was added to V_R for future use and has no effect in the highly-damped limit. An equation analogous to Eq. (11) is found for the imaginary part $4\pi\beta\omega_I - 2\pi s$.

QNM frequencies.— In order to obtain a closed-form expression for ω, expand $2i\delta - 4\pi\sigma_+ = \delta_0 + (m\delta_m + is\delta_s + iA_1\delta_A)\omega^{-1} + O(|\omega|^{-2})$. Here

$$\delta_j \equiv 2i \int_{C_{r,o}} V_j\, dr \; , \tag{13}$$

with $V_0 = q_0^{1/2}\Delta^{-1}$, $V_m = -a(2Mr - Q^2)\Delta^{-1}q_0^{-1/2}$, $V_s = [r(\Delta + Q^2) - M(r^2 - a^2)]\Delta^{-1}q_0^{-1/2}$, and $V_A = -q_0^{-1/2}a/2$. The integration contour $C_{r,o}$ runs from r_1 to r_2, crossing the real axis outside the event horizon. Since $r_2 = r_1^*$, $\{\delta_0, \delta_s, \delta_A, \delta_m\}$ are all real. Analytic expressions for these δ_j functions are readily found in terms of elliptic integrals.

With the above definitions we finally obtain

$$\omega = -m\widehat{\omega} - i(\widehat{\phi} + n\widehat{\delta}) \; , \tag{14}$$

where $\widehat{\omega} = \delta_m/\delta_0$, $\widehat{\delta} = 2\pi/\delta_0$, and $\widehat{\phi} = (s\delta_s + A_1\delta_A - \pi)/\delta_0$. As shown in Figures 2 and 3, these analytic results agree with the numerical calculations of [8].

Eq. (14) yields one branch of solutions $\omega_m(n)$ in the asymptotic limit. Interestingly, in the low-n regime (and in spherically-symmetric black holes) two branches of solutions are identified, for given field and black-hole parameters [13].

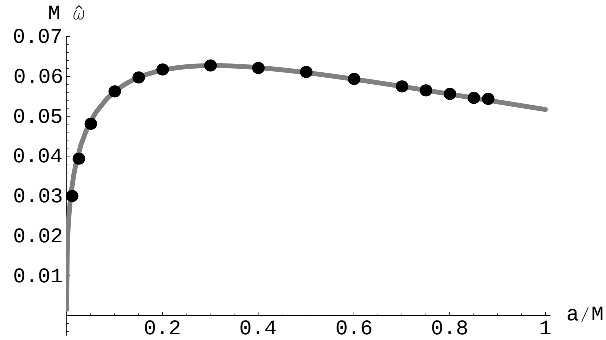

FIG. 2: The real part of the highly damped QNM frequency $\widehat{\omega}(a) = \widetilde{\omega}_R(a; m = -1)$ for $Q = 0$, according to Eq. (14) (line) and according to the numerical results of [8] (circles).

The asymptotic QNMs are not continuous at $a = 0$ [18]. For $Q = 0$, $\widehat{\omega}(a \to 0) \propto a^{1/3} \to 0$, whereas $\omega_R(a = 0) = (8\pi M)^{-1} \ln 3$. Such discontinuous behavior sometimes occurs in the Schwarzschild limit, for example in the inner structure of the black hole [14]. Note that the level spacing $\widehat{\delta}$ does continuously asymptote to the Schwarzschild result $\Delta\omega = 2\pi T/\hbar$ [7] as $\{a, Q\} \to 0$.

Discussion.— We have analytically studied the highly-damped QNM frequencies $\omega(n)$ of a rotating black hole. A Bohr-Sommerfeld-like equation for ω was derived [Eqs. (9)-(10)], analytically solved [Eq. (14)], and shown to agree and generalize previous numerical results [8] (Figures 2 and 3).

It is instructive to quantize the linear field perturbations described by the QNM [19]. A quantum of complex energy $\hbar\omega(n)$ and angular momentum $\hbar m$ may thus be associated with the highly-damped QNM frequency $\omega_m(n)$. Multiplying Eq. (10) by $\hbar$ yields

$$2 \int_{C_{t,o}} p\, dr = \left(n + \frac{1}{2} \right) h \; , \tag{15}$$

where $p = \hbar\omega V$. This equation strongly resembles the Bohr-Sommerfeld quantization rule $\oint p\, dq = (n + 1/2)h$,

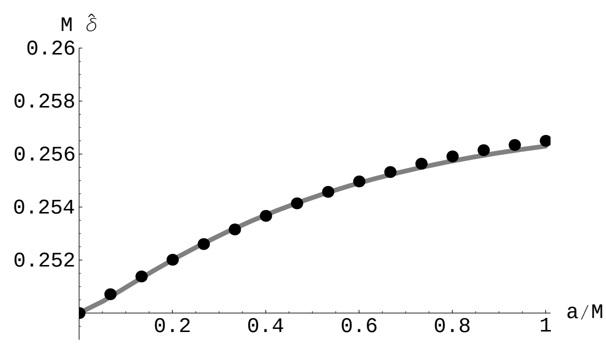

FIG. 3: Level spacing $|\Delta\omega(a)| = \widehat{\delta}$ for $Q = 0$ according to Eq. (14) (line) and the numerical fit in [8] (circles).

where p is the canonical momentum conjugate to some coordinate q, and the integration is carried out along a closed orbit. To elucidate the connection, recall that the covariant radial momentum p_r for geodesic motion of a neutral, massless particle of energy E and angular momentum p_ϕ, is given by

$$\begin{aligned}(p_r\Delta)^2 &= [(r^2+a^2)^2-a^2\Delta]E^2-2a(2Mr-Q^2)Ep_\phi \\ &\quad -(\Delta-a^2)p_\phi^2-Q_C\Delta\ ,\end{aligned} \tag{16}$$

where Q_C is Carter's (fourth) constant of motion [15]. Comparing this with Eq. (12) indicates that $V_R \approx p_r$, provided that $E=\hbar\omega$, $p_\phi=\hbar m$, and $Q_C=O(E^0)$. Hence, up to an $O(\omega^0)$ term which leads to an imaginary offset in $\omega(n)$, the integrand in Eq. (15) truly is of the form $p\,dq$ for the above QNM quantization. The implied physical content of Eq. (15) suggests that the full QNM spectrum may be determined by a generalized Bohr-Sommerfeld equation, which reduces to Eq. (15) as $\omega_I \to -\infty$. The general form of p is not uniquely determined by our highly-damped analysis. Up to $O(|\omega|^{-1})$ corrections, we may write

$$p = p_r + i\hbar s V_s + i\hbar A_1 V_A\,. \tag{17}$$

The preceding discussion implies that Eq. (15) can be interpreted as a complex version of the Bohr-Sommerfeld quantization rule. This rule was used in (the old) quantum mechanics to determine the quantum-mechanically allowed trajectories, as well as the quantized values of the associated constants of motion. Realizing the full meaning of Eq. (15) may well require a quantum theory of gravity. Conversely, this equation can possibly be used to constrain and shed light on the theory.

The quantum manifestation of a QNM may be complicated. A simple example is motivated by the outgoing boundary conditions of the QNMs and the symmetry of their frequencies $\omega_{-m}=-\omega_m^*$ [13], evident in Eq. (14). These suggest that a quantum pair of opposite angular momentum may fundamentally correspond to a QNM; a positive energy quantum escaping to infinity and a negative energy quantum falling into the black hole, in resemblance of Hawking's semiclassical radiation. Under such circumstances, a quantum process corresponding to a QNM changes the black-hole mass by $\Delta M=\hbar\omega_R$ and its angular momentum by $\Delta J=\hbar m$. For such small changes in the black-hole parameters, the corresponding change in its entropy, $\Delta S=T^{-1}(\Delta M-\Omega\Delta J)$, is given directly by Eq. (11), which we may now write as

$$\hbar\Delta S = \Delta A/4 = \Re\left(2i\int_{C_{t,i}} p_r\,dr\right)\ . \tag{18}$$

This is another indication of the adiabatic invariance of the area/entropy [3].

We thank A. Neitzke, J. Maldacena, P. Goldreich and J. Bekenstein for helpful discussions. U.K. is supported by the NSF (grant PHY-0503584).

[1] R. Ruffini and J. A. Wheeler, Physics Today, **24**, 30 (1971).

[2] D. Christodoulou, D., Phys. Rev. Lett. **25**, 1596 (1970); D. Christodoulou and R. Ruffini, Phys. Rev. D **4**, 3552 (1971).

[3] J. D. Bekenstein, Lett. Nuovo Cimento **11**, 467 (1974); J. D. Bekenstein, Phys. Rev. D **7**, 2333 (1973).

[4] For a review see H. P. Nollert, Class. Quantum Grav. **16**, R159 (1999).

[5] L. Motl and A. Neitzke, Adv. Theor. Math. Phys. **7**, 307 (2003).

[6] S. Hod, Phys. Rev. Lett. **81**, 4293 (1998).

[7] L. Motl, Adv. Theor. Math. Phys. **6**, 1135 (2003).

[8] E. Berti, V. Cardoso, and S. Yoshida, Phys. Rev. D **69**, 124017 (2004).

[9] S. A. Teukolsky, Phys. Rev. Lett. **29**, 1114 (1972).

[10] A. L. Dudley and J. D. Finley III, J. Math. Phys. **20**, 311 (1979).

[11] E. Berti, V. Cardoso, and M. Casals, Phys. Rev. D **73**, 024013 (2006); R. A. Breuer, M. P. Ryan and s. Waller, Proc. R. Soc. Lon. A **358**, 71 (1977).

[12] N. Fröman and P.O. Fröman, JWKB approximation: Contributions to the Theory, Amsterdam: North Holland 1965.

[13] E. W. Leaver, Proc. R. Soc. Lond. A **402**, 285 (1985).

[14] S. W. Hawking and G. F. R. Ellis, The Large Scale Structure of Space Time, Cambridge Univ. Press (1973); S. Hod and T. Piran, Phys. Rev. Lett. **81**, 1554 (1998) and the references therein.

[15] B. Carter, Phys. Rev., **174**, 5, 1559 (1968).

[16] Eq. (8) can also be derived as in Ref. [5], by solving for $\widehat{R}$ near the the turning points where $V_1 \simeq -(5/36)(z-z_i)^{-2}$.

[17] Using $\int_{r_1}^{r_2} i|f|dr \in \mathbb{R}$. The integration endpoints $\{t_i\}$ and $\{r_i\}$ may be used interchangeably, as $q_0(t_i)=0$ ensures that the resulting $O(|\omega|^{-1})$ correction terms vanish.

[18] The analysis is valid only for $0<a^2<M^2-Q^2$. It does not apply for $a=0$, where r_1 and r_2 coalesce to 0, nor in the extremal case $M^2-a^2-Q^2=0$, where r_- and r_+ merge to cut off the anti-Stokes line l_2. It does apply in the extremal limit, where numerical calculations fail and we find $\widehat{\omega}(a\to M)\simeq 0.051704/M$.

[19] The analysis can alternatively proceed in the geometrical optics approximation, where radiation follows null geodesics.